



Electrical conductivity of OH-bearing omphacite and garnet in eclogite: the quantitative dependence on water content

Hanyong Liu¹ · Qiao Zhu¹ · Xiaozhi Yang¹

Received: 3 April 2019 / Accepted: 5 June 2019 / Published online: 11 June 2019
© Springer-Verlag GmbH Germany, part of Springer Nature 2019

Abstract

Eclogite is potentially an important constituent in local regions in the deep crust and upper mantle. The electrical conductivity of omphacite and garnet in eclogite has been measured at 1 GPa and 350–800 °C with pre-annealed OH-bearing samples. The conductivities were determined using a piston–cylinder apparatus and a Solartron-1260 Impedance/Gain Phase Analyser in the frequency range of 10⁶–1 Hz. The sample water contents show almost no change before and after the experimental runs. The conductivity of both omphacite and garnet increases with temperature, and the activation enthalpy is ~82 kJ/mol for omphacite and 90 kJ/mol for garnet, which is nearly independent of water content in each mineral. The conduction is probably dominated by protons, and for both minerals, the conductivity increases linearly with water content, with a water content exponent of ~1. These data are used to model the bulk conductivity of an eclogite with different water contents and modal compositions. In combination with reported data, the conductivity of the eclogite is similar to that of typical granulites above 600 °C, but is much larger than that of olivine, assuming small to moderate water contents. This would mean that the contribution of eclogites, if present, to the electrical structure of the deep continental crust cannot be easily separated from that of granulites, and that the regional enrichments of eclogites in the upper mantle may cause high electrical anomalies. The results also provide information for the electrical property of orogen-related thickened deep crust where eclogites may be locally abundant, e.g., in the Dabieshan region and the Tibet plateau. At mantle depths, eclogitized portions of subducted slabs are usually of very low conductivities as suggested by geophysical observations, implying small water contents in the constitutive omphacite and garnet and the limited ability of these minerals in recycling water into the deep mantle.

Keywords Electrical conductivity · Water · Omphacite and garnet · Eclogite · Deep water cycling · Experimental studies

Introduction

There are lines of evidence favoring the regional enrichments of eclogites inside the Earth. First, the recycling of crustal materials by subduction could cause the presence of eclogite in the deep crust and upper mantle, as commonly documented for exhumed ultrahigh-pressure (UHP) terrane rocks from continental–continental collision regions (Austrheim 1991). Second, the prograde metamorphism of granulites in the thickened deep crust can lead to the formation of

eclogites, and the delamination of such crust may have been an important mechanism in losing crustal materials into the mantle and in producing an intermediate composition of the bulk continental crust (Kay and Mahlburg-Kay 1991). Third, some eclogites, especially those of xenoliths captured by kimberlites, may form by the accumulation of melts and/or the interaction of depth-derived melts with peridotites (Anderson 2007), although a general consensus on the petrogenesis has not been reached (Jacob 2004). Consequently, eclogite may affect greatly the electrical structure and other physical properties of regional zones in the deep crust and upper mantle. This topic has not received much attention, in spite of considerable efforts that have been contributed to the possible role of eclogites in producing some geochemical features of deep-seated samples (e.g., Yaxley and Green 1998).

Eclogite consists mainly of omphacite and garnet. Although nominally anhydrous, these minerals commonly

Communicated by Jochen Hoefs.

✉ Xiaozhi Yang
xzyang@nju.edu.cn

¹ State Key Laboratory for Mineral Deposits Research, School of Earth Sciences and Engineering, Nanjing University, Nanjing 210023, People's Republic of China

contain some water as OH groups bound in the lattice, and the water contents could be more than ~1500 ppm H₂O (Katayama and Nakashima 2003; Xia et al. 2005; Katayama et al. 2006; Sheng et al. 2007). These contents are virtually the highest in nominally anhydrous minerals (NAMs) derived from the crust and upper mantle (Ingrin and Skogby 2000). On the other hand, it has been established that the electrical property of NAMs is greatly enhanced by even trace amounts of water (Karato 1990; Huang et al. 2005; Wang et al. 2006; Yoshino et al. 2008, 2009; Dai and Karato 2009; Poe et al. 2010; Yang et al. 2011, 2012; Yang and McCammon 2012; Zhao and Yoshino 2016). Therefore, the electrical conductivity of water-bearing omphacite and garnet in eclogite, and thus of eclogite itself, and especially the dependence on water content deserve a thorough study for insights into the fine structure of the deep crust and upper mantle. However, this has so far not been reported.

In this study, we have in situ determined the electrical conductivity of water-bearing omphacite and garnet in eclogite at high-pressure and high-temperature conditions, and we have paid particular attention to addressing the quantitative dependence of conductivity on water content. We show that, given other conditions, the conductivity of these minerals increases greatly with increasing water content. We then model the bulk conductivity of eclogite as a function of water content and modal mineral composition. The results are important for understanding the electrical structure of the deep crust and upper mantle (at least in local zones) and the recycling of water into the mantle by omphacite and garnet in subducted eclogites.

Experiments and analytical methods

Samples

The electrical property of Earth materials is sensitive to the constitutive species, in particular those important in charge transfer, and the prevailing thermodynamic factors such as temperature. Instead, the tectonic settings (or localities) where the materials are obtained have no impact on the electrical behavior given other conditions. Thus, a fresh eclogite sample from Weissenstein, Münchberger Gneiss

Massif (Germany), was chosen as the starting material; note that the eclogite outcrops in that region were related to slab subduction and exhumation (Franz et al. 1986). The eclogite consists of medium-grained omphacite and garnet, as well as <1% (by volume) phengite and other accessory minerals. Eclogites from the world, either of terrane or xenolith forms, commonly contain impurities such as hydrous phases, fluid/mineral inclusions and/or grain boundary melts, which affect strongly the analyses of conductivity. In addition, the distribution of water (OH species) is highly heterogeneous even within sub-grain scales in the dominant omphacite and garnet in natural eclogites, which was possibly caused by limited mobilities and interactions of fluids with the eclogite minerals (Xia et al. 2005; Sheng et al. 2007). Therefore, natural eclogites are not suitable for direct measurements of the conductivity and especially the quantitative dependence on water, for which a priority is the equilibrium distribution of the species (including water). This would be more meaningful if we consider that, for conductivity runs at high pressure, the samples are very small and the core drillings of natural eclogites could lead to biased sampling concerning the mineral mixing/textures, which adds further complexity to the work.

We thus adopted the following strategy: first, omphacite and garnet grains were separated from the starting eclogite; second, omphacite and garnet samples were pre-annealed for different water contents; third, the conductivity of omphacite and garnet and the effect of water were quantitatively determined; last, the bulk conductivity of eclogite as a function of water content was modeled. This approach has been frequently used in recent years for documenting the electrical property of a rock consisting of different minerals (e.g., Xu et al. 2000b; Yang et al. 2012; Zhao and Yoshino 2016). The key, or the prerequisite, of this approach is that the studied minerals are chemically in equilibrium concerning their major/minor element. The starting eclogite was mechanically crushed, and high-quality grains of omphacite and garnet were carefully separated by hand picking under a binocular microscope. The hand-picked grains were usually 100–700 μm. The composition of each mineral is homogeneous (Table 1) and is representative of omphacite/garnet in natural eclogites (especially Fe that affects greatly the conductivity of dry minerals: see below), according to

Table 1 Composition of omphacite and garnet in the starting eclogite

Minerals	SiO ₂	TiO ₂	Al ₂ O ₃	FeO	MnO	MgO	CaO	Na ₂ O	K ₂ O	Total
Omphacite	55.64	0.07	11.38	4.27	0.02	8.44	12.98	7.31	<0.01	100.11
	<i>0.16</i>	<i>0.03</i>	<i>0.35</i>	<i>0.28</i>	<i>0.02</i>	<i>0.17</i>	<i>0.40</i>	<i>0.24</i>	<i><0.01</i>	
Garnet	37.64	0.03	22.73	26.55	0.74	6.81	5.63	0.03	<0.01	100.16
	<i>0.20</i>	<i>0.02</i>	<i>0.12</i>	<i>0.36</i>	<i>0.08</i>	<i>0.17</i>	<i>0.32</i>	<i>0.02</i>	<i>0.01</i>	

Data are the average of multi-points analyses on different grains, assuming all Fe as FeO, and data in italics are the standard deviation

available data for terrane and xenolith eclogites from the world (“Appendix”). Homogenization of the grain water content and the preparation of samples with different water contents were conducted by H annealings at elevated conditions. Since omphacite and garnet in natural eclogites commonly contain some water (Katayama and Nakashima 2003; Xia et al. 2005; Katayama et al. 2006; Sheng et al. 2007), only OH-bearing samples were prepared.

The H annealings were carried out with the hand-picked mineral grains in an end-loaded piston–cylinder press, using Ni capsules (outer diameter, 5.0 mm; inner diameter, 4.2 mm; length, 10.0 mm) plus a few weight (wt.) percent distilled water. The capsule became mechanically sealed upon compression in the press. Through this, oxygen fugacity (fO_2) in the experiments was buffered by Ni–NiO ($Ni + H_2O = NiO + H_2$). The annealings were performed at 650–700 °C and 1–3.5 GPa for a long duration of 150–180 h. The content and the homogeneous distribution of water in the annealed grains of each sample were carefully examined by Fourier-transform infrared (FTIR) spectroscopy. The grains were then crushed and ground into powder, usually ~30 to 80 μm in size, with an agate mortar and pestle under alcohol. The powder was dried in an oven and cold-pressed into a cylinder of ~1.7 mm in length and 3.0 mm in diameter for subsequent conductivity runs, which yielded a dimension factor, the ratio of sample length to cross-section area (L/S , see below) of ~240. It has been experimentally shown that, for lattice conduction in silicate minerals, the effect of grain size is negligible for a size > 5 μm , which is typical in the Earth’s interior (Yang and Heidelberg 2012). Therefore, the results of our experiments on fine powder materials can be applied directly to the deep Earth.

FTIR spectroscopy

The species and content of water in the omphacite and garnet samples prior to and after the conductivity experiments were analyzed by FTIR spectroscopy. For omphacite that is optically anisotropic, the pre-annealed samples were analyzed by polarized measurements along three orthogonal directions of a polished crystal for each sample, as suggested by Shuai and Yang (2017). For omphacite after conductivity runs which are characterized by very small grains and for cubic garnet, the water contents were measured by unpolarized analyses of > 15 randomly oriented crystals in each sample, of which the average was used to calculate the content following the work of Qiu et al. (2018).

Transmission FTIR spectra were obtained using a Hyperion 2000 microscope coupled to a Bruker Vertex 70 V spectrometer. Instrumental and analytical details were as follows: a Global source, a Ge–KBr beam splitter, a liquid nitrogen cooled mercury–cadmium–telluric (MCT) detector, a square aperture of $60 \times 60 \mu\text{m}$, a resolution of 4 cm^{-1} , and a total

of 128 scans for each spectrum. A wire-grid Ze–Se polarizer was used to produce polarized IR radiation. Fractures were avoided, and the FTIR measurements were usually performed on optically clean areas. For the analyses, the optics were always kept under vacuum for the spectrometer and were continuously purged by purified CO_2 – and H_2O -free air for the microscope. A baseline correction was applied to each spectrum with a spline fit method, and the total absorbance was integrated in the range of ~3700 to 3200 cm^{-1} . H_2O contents of the studied samples were estimated by employing the mineral-specific integral absorption coefficients reported for omphacite and garnet in eclogite (Katayama et al. 2006). The uncertainty of H_2O contents is less than 10% relative for the polarized analyses (Shuai and Yang 2017), and is within 10–20% relative for the unpolarized analyses (Qiu et al. 2018).

Impedance measurements

Usually, eclogites form at > 1 GPa and over a range of temperature. Natural eclogites, e.g., due to the subduction and exhumation of slabs, can be present from the shallow crust (1 to several bars) to the deep mantle (> 3 GPa). It has been shown that pressure has a small effect on the conductivity of silicate minerals (e.g., Xu et al. 2000a; Dai and Karato 2009; Poe et al. 2010). Consequently, the conductivity measurements were carried out at 1 GPa with an end-loaded piston–cylinder press. By this, relatively large samples could be used, and the uncertainty of sample dimensions could be greatly reduced (note that the smaller the sample, the greater is the uncertainty from sample distortions/sample–electrode contacts).

Because of the semi-conductor behaviors of Earth materials at elevated conditions, their conductivity should be analyzed by impedance spectroscopy. The impedance spectra were measured with a Solartron 1260 Impedance/Gain Phase Analyser, by frequency sweeping from 10^6 to 1 Hz at 0.5 V applied voltage. The assembly design, Fig. 1, follows that in our previous work (Yang et al. 2011, 2012; Yang 2012; Yang and Heidelberg 2012; Yang and McCammon 2012; Li et al. 2016, 2017; Liu et al. 2019).

In brief, a double-capsule design was employed, including a U-shape Ni capsule in which the sample enclosed by a highly resistive, soft and hexagonal boron nitride (BN) capsule, two Pt electrodes, Ni–NiO buffer pairs and an S-type thermocouples were carefully placed. Subduction zones are in general oxidizing (Frost and McCammon 2008), so we used the Ni–NiO buffer. Ni electrodes were not employed, because the formation and occurrence of NiO powder along the sample–electrode interfaces would block charge transfer and affect conductivity analyses. Pt reacts with Fe at high temperature, leading to gradual Fe loss in minerals if the run duration is long; however, it has been shown by Yang

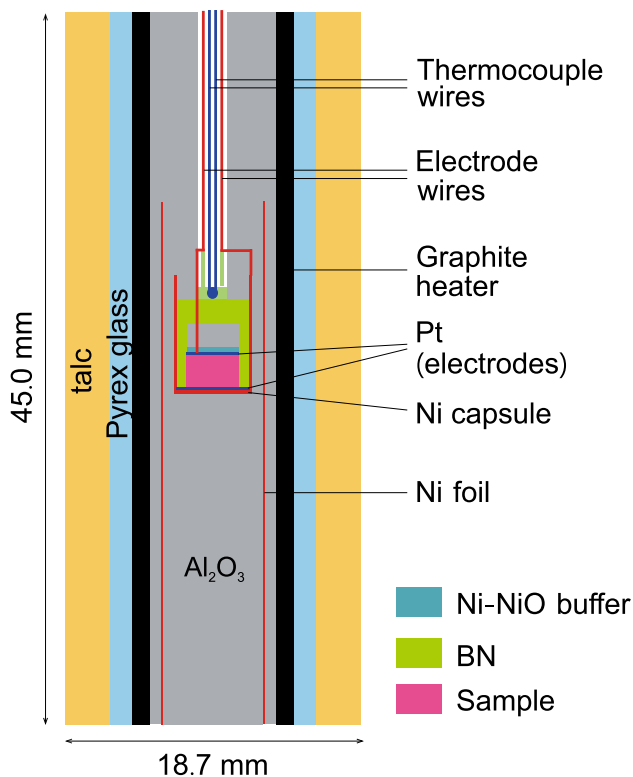


Fig. 1 Sample assembly for electrical conductivity measurements. A shielding Ni foil was located between the sample and (graphite) heater

et al. (2011) that, for conductivity runs at < 1000 °C and with short run durations (~ 1 min per impedance analysis), the reaction is insignificant (supported also by the reproducible conductivities between different heating–cooling cycles: see below). BN itself does not affect the redox state, but the reaction of BN with O_2 , by $4BN + 3O_2 = 2B_2O_3 + 2N_2$, yields reduced conditions. This reaction is important when O_2 is abundant (e.g., in air) and at long durations beyond ~ 1000 °C (Wendlandt et al. 1982). For conductivity runs with the relatively sealed design of Fig. 1 and at low temperature, BN plays a negligible role in redox buffering, evidenced by the careful Fe^{3+} analyses on Fe-containing samples so that their Fe^{3+}/Fe^{2+} ratios are well buffered (Yang et al. 2011, 2012; Yang and McCammon 2012). Therefore, the double-capsule design helps to maintain sample geometry and produces a closed chamber upon gradual hot pressing (note that BN has very low permeability for molecular water and hydroxyl ions). This is helpful in minimizing sample distortions, buffering fO_2 in the system, and avoiding the diffusion of graphite (heater) through pressure media into samples.

Before sample assembly, the Al_2O_3 parts were pre-heated at 1000 °C for 4 h to remove absorbed water, and during assembly no cement/glue was used to immobilize the various parts to avoid volatile releasing at elevated temperatures.

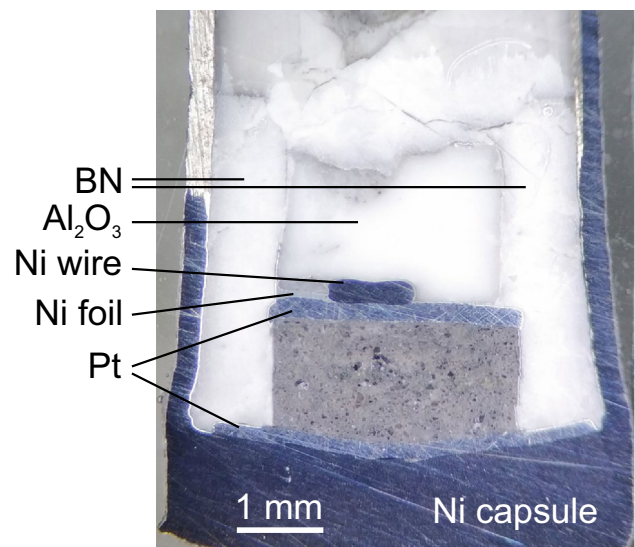


Fig. 2 A representative recovered sample after conductivity run (B174, garnet). Different colors of the sample are due to different grain sizes and sample loss during polishing

After the assembly was finished, it was heated in an oven at 136 °C for ~ 24 h, and after the assembly was loaded into the press and the pre-set pressure was reached, the sample was heated at ~ 200 °C for a few hours and then heated to ~ 500 to 600 °C for various durations. The impedance spectra were recorded in different heating–cooling cycles. The measurements were conducted at 350–800 °C, to minimize the diffusion loss of water in the samples. After conductivity runs, the recovered samples were polished for optical examinations and FTIR analyses. A representative cross section of a recovered sample is shown in Fig. 2. In general, the Ni–NiO pairs were present, and the sample distortions were usually negligible. The absolute sample dimensions changed after the runs, but the changes are expected to be small to negligible after the compression at 1 GPa and the pre-heating to 500–600 °C in the first heating cycle. The effective length (L) and cross-sectional area (S) of the recovered samples, by taking into account the contact between the sample and electrodes, were used to obtain the conductivity (σ) by $\sigma = L/SR$, where R is the resistance by fitting the impedance arc in the high-frequency range as commonly used in the community (see below). As argued in our early work, the uncertainty is < 20 °C for temperature and is usually $< 10\%$ relative for the final conductivity (Yang et al. 2011, 2012; Yang 2012; Yang and McCammon 2012).

Results

Representative FTIR spectra of the pre-annealed omphacite and garnet samples are present in Fig. 3, and the spectra generally show H-related absorption bands at 3700–3000 cm^{-1} .

For omphacite, the dominant bands centered at ~ 3465 , 3500 and 3620 cm^{-1} , and for garnet, the most significant band was observed at $\sim 3630\text{ cm}^{-1}$ plus small shoulder peaks at ~ 3600 and 3660 cm^{-1} . These are typical of OH groups in natural omphacite and garnet (Katayama and Nakashima 2003; Xia et al. 2005; Katayama et al. 2006; Sheng et al. 2007). The H_2O contents are ~ 85 , 150 and 290 ppm for the pre-annealed omphacite samples, and are ~ 40 and 100 ppm for the pre-annealed garnet samples. The H_2O contents of the samples after conductivity runs show nearly no change (Table 2), in particular when the uncertainty is considered. It is thus reasonable to expect that any obvious changes in the composition of other major/minor elements, which are much more sluggish than H, are unlikely in the runs. Representative impedance spectra of the samples are illustrated in Fig. 4. The spectra usually show an arc in the high-frequency range and a short tail in the low-frequency range, although the tail is sometimes not obvious at low temperature. The general features of the spectra are consistent with available reports for various silicate minerals (Huebner and Dillenburg 1995; Huang et al. 2005; Romano et al. 2006; Wang et al. 2006;

Yoshino et al. 2008, 2009; Dai and Karato 2009; Poe et al. 2010; Yang et al. 2011, 2012; Yang 2012; Yang and Heidelbach 2012; Yang and McCammon 2012; Li et al. 2016, 2017; Zhao and Yoshino 2016). The high-frequency arc is commonly attributed to grain interior lattice conduction, and the short tail is usually ascribed to interactions between the sample and electrodes (electrode effects).

Electrical conductivity (σ) of silicate minerals at elevated conditions can be described by the Arrhenius equation:

$$\sigma = A_0 \cdot \exp\left(-\frac{\Delta H}{RT}\right), \quad (1)$$

where A_0 is a pre-exponential constant, ΔH is the activation enthalpy, R is the gas constant and T is temperature (K). In the initial heating, the conductivity analyses were sometimes influenced by residual moisture and/or non-equilibrium issues in the system, producing data deviating from those in subsequent heating-cooling cycles and not obeying Eq. (1) as observed in similar studies (Yang et al. 2011; Yang and Heidelbach 2012; Li et al. 2016, 2017; Liu et al. 2019). The affected data were excluded. The measured conductivities

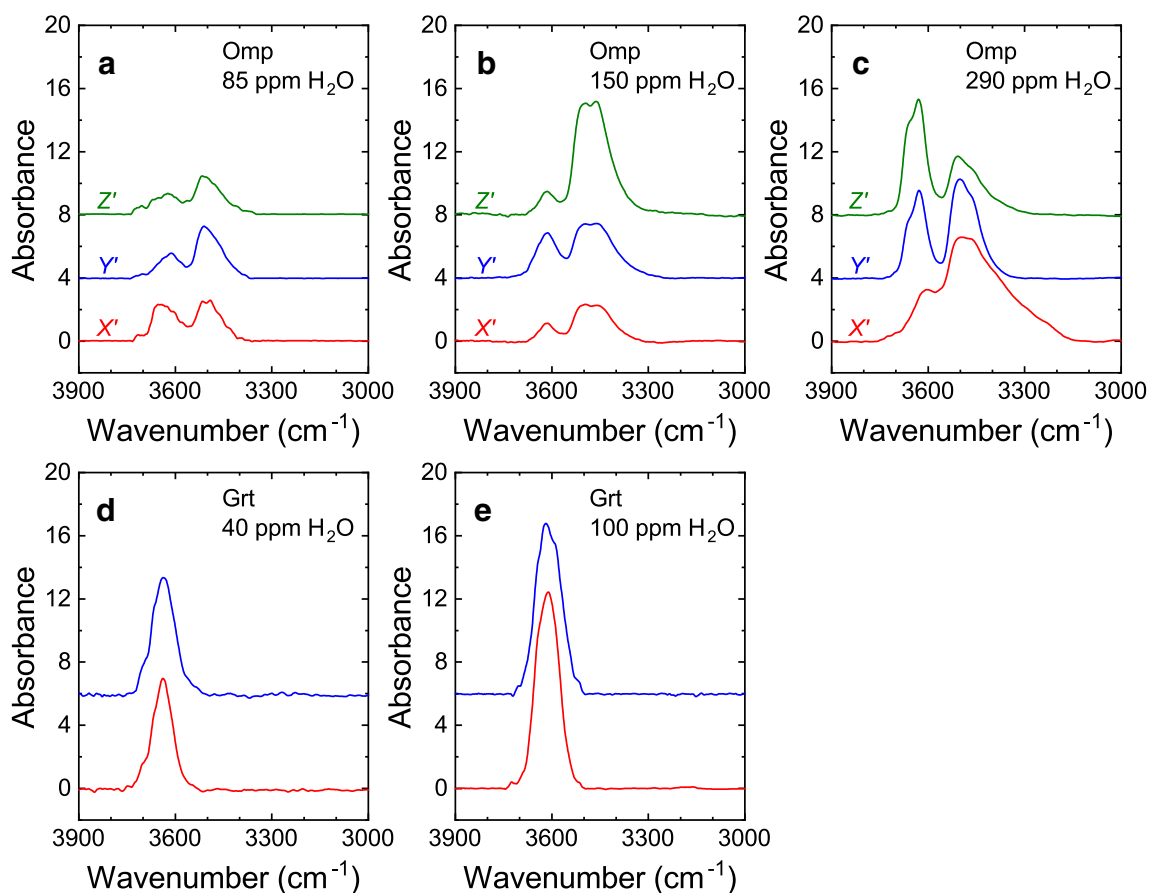


Fig. 3 Representative FTIR spectra of pre-annealed omphacite and garnet samples. **a–c** Polarized spectra for omphacite along three orthogonal directions of each same crystal (X' , Y' and Z') and **d**, **e**

unpolarized spectra for garnet (different grains). The spectra were normalized to 1 cm thickness and vertically offset. *Omp* omphacite, *Grt* garnet

Table 2 Summary of samples and fitting parameters

Run no.	ppm H ₂ O		<i>L/S</i> (m ⁻¹)	log ₁₀ (A ₀ (S/m))	log ₁₀ (A (S/m))	<i>r</i>	Δ <i>H</i> (kJ/mol)	Δ <i>H</i> _H (kJ/mol)
	Initial	Final						
<i>Omphacite</i>								
B185	85	80	269	1.38 ± 0.24			84 ± 4	
B149	150	160	216	1.52 ± 0.14			82 ± 2	
B145	290	300	290	1.75 ± 0.12			81 ± 2	
Multi-linear fitting					3.51 ± 0.11	1.10 ± 0.04		82 ± 1
<i>Garnet</i>								
B167	40	45	226	1.80 ± 0.17			90 ± 3	
B174	100	95	245	2.26 ± 0.12			91 ± 2	
Multi-linear fitting					4.37 ± 0.24	1.07 ± 0.09		90 ± 2

Sample H₂O contents were rounded to the nearest 5 ppm. *L/S* represents the ratio of the effective length to cross-sectional area of the recovered samples (the initial *L/S* is ~240, see text). Parameters were obtained by linear fittings for each run and multi-linear fittings for all data of each mineral

are much greater than the assembly background conductivity (Fig. 5), as assessed in our early work (Yang et al. 2011). The conductivity data of the samples and their fittings are shown in Fig. 5, and the parameters by fitting the data to Eq. (1) are summarized in Table 2. The data are reproducible between different heating–cooling cycles of each sample, suggesting the absence of system hysteresis and the negligible role of Fe loss from sample to Pt. The activation enthalpy is 81–84 kJ/mol for omphacite and ~90 kJ/mol for garnet. The results demonstrate that, in general, the conductivity increases with increasing temperature/water content, agreeing well with available reports for other NAMs (Huang et al. 2005; Wang et al. 2006; Yoshino et al. 2008, 2009; Dai and Karato 2009; Poe et al. 2010; Yang et al. 2011, 2012; Yang 2012; Yang and McCammon 2012; Zhao and Yoshino 2016).

Concerning the OH-bearing omphacite/garnet, the measured conductivity is actually the sum of two different parts: $\sigma = \sigma_{\text{dry}} + \sigma_{\text{H}}$, where σ_{dry} is the conductivity of the mineral at dry status and σ_{H} is the conductivity dominated by water (Huang et al. 2005; Wang et al. 2006; Yoshino et al. 2008, 2009; Dai and Karato 2009; Poe et al. 2010; Yang et al. 2011, 2012; Yang and McCammon 2012; Zhao and Yoshino 2016). Usually, σ_{dry} is much smaller than σ_{H} at low temperature (see “Conduction mechanism”), so that σ can be approximated by σ_{H} . For a quantitative evaluation of the influence of water on the conductivity, the data are further processed by:

$$\sigma = A \cdot C_{\text{H}}^r \cdot \exp\left(-\frac{\Delta H_{\text{H}}}{RT}\right), \quad (2)$$

where *A* is a constant, *C_H* is water content, *r* is a factor linked to the nature of charged H species, and Δ*H_H* is activation enthalpy. This assumes that the conduction in both the OH-bearing omphacite and garnet is dominated by water (H, see

below). It should be noted that *r* is physically different from the water content exponent in the solubility law that is used to describe water dissolution in NAMs, and cannot be used to predict the mechanism of water incorporation (e.g., Huang et al. 2005; Wang et al. 2006; Yoshino et al. 2008; Dai and Karato 2009; Poe et al. 2010; Yang et al. 2011, 2012; Yang and McCammon 2012; Zhao and Yoshino 2016). Parameters by multi-linear regression fittings of all the data of each mineral to Eq. (2) are given in Table 2. The activation enthalpy is ~82 and 90 kJ/mol for omphacite and garnet, respectively, and the exponent *r* is ~1 for both minerals.

Conduction mechanism

In the Arrhenius plots of the measured conductivities, the slope is indicative of activation enthalpy, and the difference in slopes would imply different conduction mechanisms. The absence of any apparent changes or kinks in the slope of our measured data for omphacite or garnet suggests the absence of any changes in the conduction mechanism of each run. The virtually same activation enthalpy (slope) of each mineral at different water contents would then indicate that, for each mineral, the electrical conduction was dominated by the same mechanism. For OH-absent (dry) minerals containing Fe²⁺ and Fe³⁺, the conduction is usually attributed to small polarons, e.g., by the hopping of electron holes between Fe²⁺ and Fe³⁺. For OH-present (wet) minerals containing Fe²⁺ and Fe³⁺, small polarons related to Fe and protons related to OH groups both contribute to bulk conductivity. Because of the high mobility of H, the contribution of proton conduction is usually more significant than that of small polaron conduction (especially at relatively low temperature), as argued for other NAMs (Yoshino et al. 2008, 2009; Dai and Karato 2009; Poe et al. 2010; Yang et al. 2011, 2012; Yang

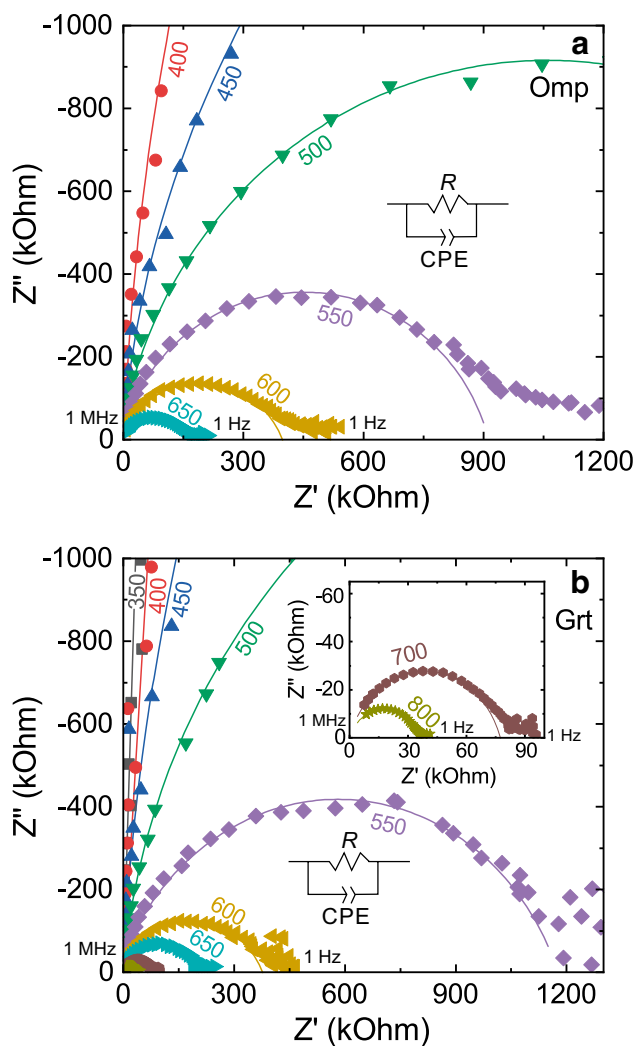


Fig. 4 Representative complex spectra for **a** omphacite (B145) and garnet (B174). Z' and Z'' are the real and imaginary parts of the complex impedance, respectively. The frequency decreases along the Z' -axis from left (1 MHz) to right (1 Hz). An equivalent circuit of a single R -CPE circuit element, a resistor R and a constant phase element (CPE) in parallel, was used to fit the spectra in the high-frequency range. The short tail in the low-frequency region and the offset from the origin were not included. Inset in **b** shows the spectra at 700 and 800 °C. The numbers close to the spectra are temperatures in °C

and McCammon 2012; Zhao and Yoshino 2016). Therefore, the electrical transfer in our samples is controlled mainly by protons.

Our data demonstrate that, for each mineral, the activation enthalpy of proton conduction is nearly independent of water content (Fig. 5). This agrees well with recent observations and arguments for proton conduction in other NAMs (Yoshino et al. 2008, 2009; Yang et al. 2011, 2012; Yang and McCammon 2012; Zhao and Yoshino 2016; Li et al. 2017). Poe et al. (2010) have observed similar independence for wet olivines with less than ~800 ppm H₂O, however, their H-enriched samples (> 1000 ppm H₂O) show much smaller

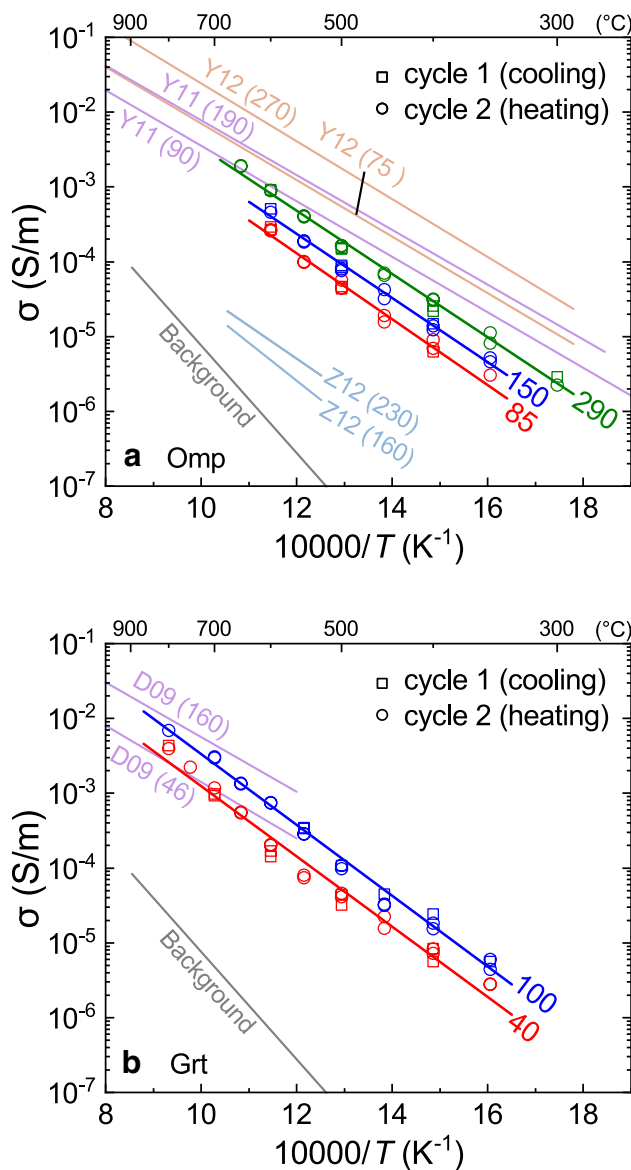


Fig. 5 Electrical conductivity of **a** omphacite and **b** garnet. Lines are from linear regression of measured data. Water contents (ppm H₂O) of the samples are also shown, including those in parentheses. Compiled data: Y12, Yang and McCammon (2012) for mantle augite at 1 GPa; Y11, Yang et al. (2011) for lower crustal diopside at 1 GPa; Z16, Zhao and Yoshino (2016) for mantle diopside at 1.5 GPa; D09, Dai and Karato (2009) for majorite garnet at 8 GPa [the conductivity data of Zhao and Yoshino (2016) show change in conduction mechanism at higher temperatures, and only their data at low temperatures due to proton conduction were compiled]. Background conductivity of the assembly was taken from Yang et al. (2011)

activation enthalpies. The dependence of activation enthalpy on water content in the wet olivines of Poe et al. is inconsistent with the independence of wet olivine to 1800 ppm H₂O observed by Yoshino et al. (2009), and it seems that the H-enriched olivines of Poe et al. undergo significant dehydration, which had affected their measurements (Yoshino

et al. 2009; Yang 2012). In sharp contrast, the activation enthalpy of small polaron conduction in dry Fe-containing minerals decreases progressively with increasing Fe content (Romano et al. 2006; Yang et al. 2011, 2012; Yang and McCammon 2012; Zhao and Yoshino 2016; and references therein). The microscale mechanism of charge transfer might differ between proton conduction and small polaron conduction; however, the physical background has not been well understood. One likely model is related to the lattice position of the charge carriers, e.g., H occurs as point defects vs. Fe occupies structural sites. For small polaron conduction, the smaller activation enthalpy at elevated Fe contents might be accounted for by the enhanced transfer of electron holes between Fe^{2+} and Fe^{3+} , e.g., due to the enhanced connectivity of Fe atoms at higher Fe concentrations. For proton conduction, protons are attached to lattice O atoms by hydrogen bonds. In this case, protons may jump between any neighboring O, so that the level of lattice protonation is probably independent of the spatial relationship between the O atoms. This may produce the observed independence of activation enthalpy on water content. The mechanism of H incorporation in the structure may offer some help; however, it is not clear if all H species in a mineral contribute to conduction and if their contribution is equal (see below). Moreover, a direct link between H incorporation and H conduction appears absent: the former involves the occupation of interstitial positions (e.g., H_2O) and/or the (coupled) substitution for other cations (e.g., H^+), while the latter may be linked to the jump of H between different sites regardless of the incorporation mechanism.

For H conduction in the studied omphacite and garnet, it is unclear if the independence of activation enthalpy on water content is still valid at very H-rich conditions, because of the challenges in synthesizing those samples and in conducting conductivity runs due to easier H dehydration under otherwise comparable conditions. However, similar independence has been reported for proton conduction in majorite garnet with up to ~ 420 ppm H_2O (Dai and Karato 2009), wadsleyite with up to $\sim 12,000$ ppm H_2O (Yoshino et al. 2008), olivine with up to ~ 1800 ppm H_2O (Yoshino et al. 2009) and diopside (clinopyroxene) with up to ~ 2000 ppm H_2O (Zhao and Yoshino 2016). It is thus reasonable to expect similar results for the omphacite and garnet with small to moderate water contents. The activation enthalpy of proton conduction in omphacite and garnet, ~ 80 to 90 kJ/mol (Table 2), is much smaller than that of proton diffusion in clinopyroxene and garnet, 120 – 330 kJ/mol (Ingrin and Blanchard 2006). The different activation enthalpies between these transport processes are consistent with the arguments documented for other NAMs (Huang et al. 2005; Wang et al. 2006; Yoshino et al. 2008, 2009; Dai and Karato 2009; Poe et al. 2010; Yang et al. 2011, 2012; Yang 2012; Yang and McCammon 2012; Zhao and

Yoshino 2016). Very likely, the mobility of H is different between conduction and diffusion experiments. This would imply that, for NAMs, the experimentally measured H diffusion coefficients cannot be simply used to estimate the conductivity due to H conduction. The exponent r is ~ 1 for both omphacite and garnet, agreeing with recent studies for H conduction in other NAMs (e.g., Yang et al. 2011, 2012; Yang and McCammon 2012; Zhao and Yoshino 2016; Li et al. 2017). In contrast, few early studies reported r of ~ 0.7 (Huang et al. 2005; Wang et al. 2006), which may have been related to relatively large uncertainties in those experiments. The r value of ~ 1 does not necessarily mean that all H in the lattice contributes equally to conduction. Instead, it may simply imply that the amount of charged H is proportional to the bulk water content.

Comparison with available work

In Fig. 5, the conductivities of OH-bearing clinopyroxene (diopside and augite) and garnet (majorite garnet) samples from previous studies were compiled for a comparison with our data of omphacite and garnet in eclogite. For convenience, only samples with comparable water contents are considered.

For clinopyroxene with similar H_2O contents (Fig. 5a), the conductivity is similar between crustal diopside in granulite (Yang et al. 2011) and mantle augite (Yang and McCammon 2012). In contrast, the conductivity of omphacite, although much larger than that of mantle diopside in peridotite (Zhao and Yoshino 2016), is smaller. For each of these samples, the bulk conductivity includes the contribution from conduction by both small polarons and protons, although the role of the latter is more significant. The conductivity runs of these studies were carried out at similar pressures, 1 and 1.5 GPa. Accordingly, the difference in conductivity between these samples is linked to their different total Fe contents (expressed as the equivalent amount of FeO), e.g., $\sim 4.27\%$ for the omphacite (Table 1), 2.20 – 2.60% for the mantle diopside (Zhao and Yoshino 2016), and 8.20 – 8.40% for the crustal diopside and mantle augite (Yang et al. 2011; Yang and McCammon 2012). The yielded activation enthalpy differs slightly between these minerals, e.g., ~ 82 kJ/mol for omphacite (Table 2), 86 – 98 kJ/mol for mantle diopside (Zhao and Yoshino 2016), and ~ 70 kJ/mol for crustal diopside and mantle augite (Yang et al. 2011; Yang and McCammon 2012). The spectral shapes and frequency position of OH groups are different between omphacite, augite and diopside (Skogby et al. 1990). This would imply different H point defects between these minerals, which may cause different activation enthalpies if the mobility differs between different H sites.

which would not cause anisotropic conductivities by the mineral alignments, and because the conductivity is similar between omphacite and garnet under otherwise comparable conditions (Fig. 6).

With these considerations, the bulk conductivity is modeled by the Hashin–Shtrikman upper (σ_{HS+}) and lower (σ_{HS-}) bounds (Hashin and Shtrikman 1963):

$$\sigma_{HS+,HS-} = \sigma_{1,2} + f_{2,1} \cdot [(\sigma_{2,1} - \sigma_{1,2})^{-1} + f_{1,2} / (3 \cdot \sigma_{2,1})]^{-1}, \quad (3)$$

where $\sigma_{1,2}$ and $f_{1,2}$ are the conductivities and volume proportions of the two constituents, respectively. The Hashin–Shtrikman bounds offer the narrowest restrictions on the bulk property of a two-phase composite in the absence of geometrical information. We assume small to moderate water contents for the modeling, e.g., 100, 400 and 800 ppm H₂O for omphacite and 20, 80 and 160 ppm H₂O for garnet (Fig. 6), respectively, and the results are shown in Fig. 7. Given the mineral fractions, the upper and lower bounds are similar to each other under otherwise identical conditions, supporting the assumption that mineral textures do not affect the results. With increasing temperature, the upper and lower bounds become progressively closer (Fig. 7). In general, the bulk conductivity increases with increasing H₂O content in the constitutive omphacite and garnet (and thus eclogite).

The electrical conductivity of eclogite (rock) samples has been measured using impedance spectroscopy (Bagdassarov et al. 2011; Guo et al. 2014; Dai et al. 2016). The sample of Guo et al. (2014) consisted of 30% accessory phases, 30% omphacite and 40% garnet, and the conductivities, which are much larger than the values from other reports and from our modeling (Fig. 7), show a change in the conduction mechanism at ~400 °C. The starting rock of Guo et al. was not a typical and fresh eclogite, and the data were excluded from further discussion. Our modeled bulk conductivity of eclogite with 400–800/80–160 ppm H₂O for omphacite/garnet is similar to that of a wet eclogite (with unknown H₂O content) reported by Bagdassarov et al. (2011). The contents of major/minor elements (especially Fe) in the constitutive minerals are similar between these eclogites, and we expect comparable H₂O contents of minerals in Bagdassarov et al., assuming that their analyses were not affected by impurities (such as hydrous minerals) in their sample. Dai et al. (2016) have measured the conductivity of a ‘dry’ eclogite with similar mineral major/minor element contents as in our sample: their conductivities fall between our samples with 100/20 and 400/80 ppm H₂O for omphacite/garnet; however, their sample was actually not dry (see their Fig. 2). Therefore, our bulk conductivity data are not inconsistent with those of rock eclogites in available studies, where the H₂O contents and the effect of H₂O on conductivity were not quantified. Our data can thus be applied

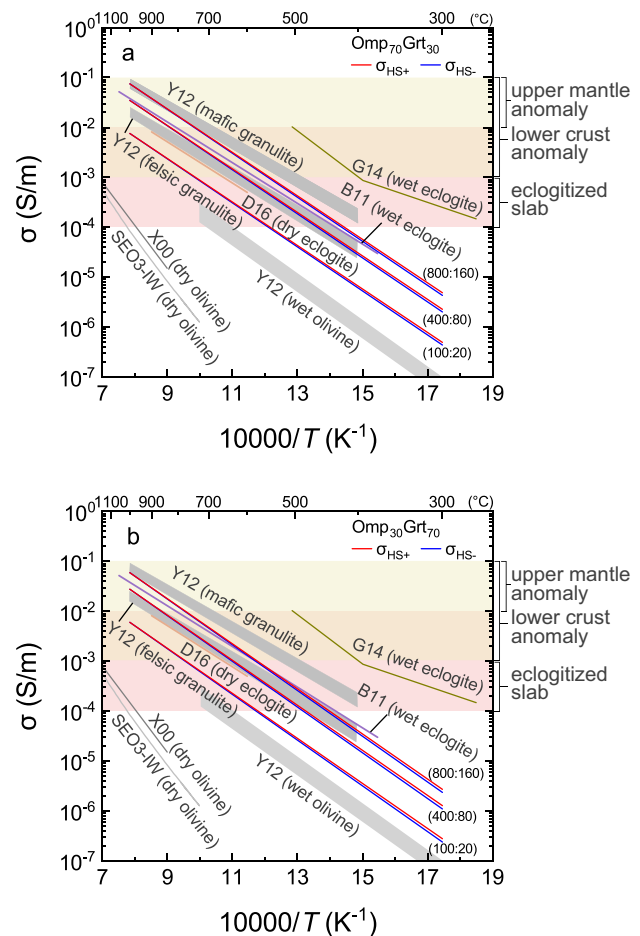


Fig. 7 Bulk conductivity of eclogite for a modal composition of **a** 70% omphacite+30% garnet and **b** 30% omphacite+70% omphacite. The assumed H₂O contents were 100, 400 and 800 ppm for omphacite and 20, 80 and 160 ppm for garnet, respectively, with a partition coefficient ($D^{Grt/Omp}$) of 0.2 (see text for details). Gray areas denote the modeled conductivity of pyroxene-rich mafic granulites and feldspar-rich felsic granulites (Yang et al. 2012) and of mantle olivine with 40–100 ppm H₂O (Yang 2012), with an exponent r of 1 for the modeling. Resolved conductivity ranges of the deep crust, upper mantle and eclogitized slabs are illustrated. Data sources: B11 (wet eclogite), Bagdassarov et al. (2011) at 2.5 GPa; Y12 (mafic/felsic granulite), Yang et al. (2012) at 1 GPa; Y12 (wet olivine), Yang (2012) at 1 GPa; G14 (wet eclogite), Guo et al. (2014) at 1.5 GPa; D16 (dry eclogite), Dai et al. (2016) at 2 GPa; X00 (dry olivine), Xu et al. (2000a) at 4 GPa; SEO3-IW (dry olivine), Constable (2006)

to the Earth’s interior, because the minerals are moderate in major/minor element contents and are small to moderate in water contents. This would make more sense if we consider the more significant influence of water on the conductivity of NAMs than that of other species, e.g., a very small change in H₂O content on ppm levels vs. a very large change in Fe content on wt % levels.

Implications for deep electrical property and deep water recycling

At 700–900 °C, the conductivity of the eclogite is 10^{-3} – 10^{-1} S/m for a H₂O content of 100–800 ppm in omphacite and 20–160 ppm in garnet (Fig. 7). Therefore, the conductivity of eclogite is quite high at small to moderate H₂O contents. Eclogite can be locally abundant in the deep crust and upper mantle, and accordingly the water-related conductivity could offer important constraints on the deep Earth, by combining with the electrical properties of other dominant materials in the deep crust and upper mantle. It should be further noted that, since omphacite and garnet are in general richer in Fe in subduction-related terrane eclogites than in volcano-related xenolith eclogites (“Appendix”), the discussion would be more meaningful for subduction-involved tectonic settings.

The lower crust in the continental regions is dominated by granulite, consisting mainly of clinopyroxene (diopside but not omphacite), orthopyroxene and plagioclase. Yang et al. (2012) have demonstrated that, for moderate concentrations of major/minor element and structural water (e.g., 400 ppm H₂O for pyroxenes and 250 ppm H₂O for plagioclase and equilibrium partitioning of elements), the conductivity of pyroxene-rich mafic granulites and plagioclase-rich felsic granulites is $\sim 10^{-3}$ to 10^{-1} S/m at deep crustal conditions, much greater than previous estimates. Given other conditions in the deep crust, the conductivity of eclogites with a H₂O content of 400–800 ppm in omphacite and 80–160 ppm in garnet is broadly similar to that of granulites (Fig. 7). This appears more reasonable if we consider that the H₂O contents of minerals in the deep crustal granulites (xenoliths) range usually from a few tens to hundreds of ppm (Yang et al. 2008). Therefore, the contribution of eclogites, if present, to the electrical nature of the deep crust cannot be easily separated from that of granulites. The lower crust in many continental areas is characterized by high conductivity of 10^{-3} – 10^{-1} S/m (Shankland and Ander 1983; Hyndman and Shearer 1989; Glover 1996), which is similar to the conductivity of OH-bearing eclogites and granulites at potential conditions. Therefore, the dominance of granulites/eclogites with reasonable mineral compositions may account for many of the geophysically observed conductivity properties of the deep crust.

In particular, our results may place some constraints on the electrical structure of the thickened deep crust below orogens. The Dabieshan region in central China is a typical UHP metamorphic belt, where crustal materials was subducted to > 80 km depths and then returned to crustal levels (Zheng 2008). Exhumed terrane eclogites,

with H₂O contents of usually a few tens to ~ 1000 ppm in the constitutive omphacite and garnet (Xia et al. 2005; Sheng et al. 2007), are widely found in that region. Magnetotelluric surveys have reported high conductivities of 10^{-3} – 10^{-1} S/m at ~ 20 to 45 km depths in many of the Dabieshan areas, along with low-conductivity zones of 10^{-4} – 10^{-3} S/m (Xu et al. 2016). The high-conductivity zones could be reasonably accounted for by the local enrichments of eclogites according to our data (Fig. 7) and/or the dominance of granulites (Yang et al. 2012). In contrast, the very resistive zones may indicate the local absence of abundant water-rich eclogites or the very low prevailing temperature, e.g., < 600 °C (Fig. 7). Similarly, high conductivities of usually 10^{-3} – 10^{-1} S/m have been resolved at ~ 40 to 90 km depths beneath the Tibetan Plateau (Wei et al. 2001), where the Indian-Asian plate collision has resulted in significant crustal thickening. Eclogite terranes have been found in Tibet, and they could occur at depths up to ~ 100 km (Giese et al. 1999). The presence of locally abundant eclogites in the Tibetan deep crust may produce the resolved high conductivity. Studies on the water contents of eclogite minerals in Tibet and the regional temperature profiles may provide further constraints on this issue.

The upper mantle is dominated by peridotite consisting mainly of olivine, orthopyroxene and clinopyroxene (diopside but not omphacite), and olivine is the most abundant mineral. Pyroxenes are usually isolated in peridotite, contributing very little to bulk conductivity, and therefore, olivine determines greatly the electrical structure of the upper mantle. The conductivity of both dry olivine and wet olivine with potential water contents in the upper mantle is usually below $\sim 10^{-3}$ S/m (Xu et al. 2000a; Constable 2006; Yang 2012; Gardés et al. 2014), which is lower than the geophysically resolved high conductivity of 10^{-2} – 10^{-1} S/m at ~ 50 to 150 km depths (Shankland et al. 1981; Evans et al. 2005). The conductivity of OH-bearing eclogite is greater by orders of magnitudes than that of olivine, depending on the H₂O content (Fig. 7). Therefore, the local presence of eclogites in the upper mantle may cause regional high conductivity. By comparison with olivine, the local presence of only a small amount of eclogites, e.g., with a volume fraction of several to $\sim 10\%$ depending on temperature and H₂O content, would raise the regional bulk conductivity to 10^{-2} – 10^{-1} S/m, and the required volume proportion would be even less if the eclogites have higher H₂O and Fe contents in the constitutive minerals. However, if the locally enriched eclogites are only on the scale of several meters to kilometers, they might not be detected by the present magnetotelluric techniques due to insufficient spatial resolution.

Subduction is important for transferring crustal materials into the deep Earth. During deep subduction, the subducted slabs would experience a series of complex reactions and phase changes. At shallow depths, the breakdown of hydrous phases such as amphibole, chlorite and serpentine would release fluids, which escape rapidly from the system due to their low density and/or interact with the surrounding wall-rocks (e.g., Manning 2004). The released H₂O may cause high conductivities in the overlying mantle wedges (Reynard et al. 2011; Manthilake et al. 2015). However, the resultant electrical anomalies are likely a transient phenomenon, since H₂O is very buoyant and the system is in fact not closed (i.e., fluids cannot be maintained for long durations). The residual crustal materials in the slabs would convert into eclogite via the so-called eclogitization. The subduction of eclogites has been considered as an important mechanism in recycling water into the deep mantle, partly due to the high H₂O contents of up to > 1000 ppm in the constitutive omphacite/garnet as found for exhumed terrane eclogites (Katayama and Nakashima 2003; Xia et al. 2005; Katayama et al. 2006; Sheng et al. 2007). The electrical conductivity of subducted slabs has not been well resolved. However, magnetotelluric models have often assumed that eclogitized slabs at > 80 km depths are highly resistive, and the conductivity, which is orders of magnitudes smaller than that of the overlying mantle wedges and the surrounding normal mantle, is $\sim 10^{-4}$ to 10^{-3} S/m. This assumption has been verified by electromagnetic studies (Chave et al. 1991) and has been widely adopted by recent studies (e.g., McGary et al. 2014; Kapinos et al. 2016). At the relevant depths, the potential temperature of the eclogitized slabs is usually 600–900 °C only (Manning 2004; McGary et al. 2014). In combination with the conductivity data (Fig. 7), we suggest that the H₂O contents of omphacite and garnet in the deep-subducted eclogite (e.g., beyond 80 km depth) should be very small, e.g., < 400 ppm for omphacite and < 80 ppm for garnet for moderate compositions in their major/minor element.

This would imply that the recycling of water into the deep mantle by omphacite and garnet in subducted eclogites is not that efficient as considered previously, and that the high H₂O contents of omphacite and garnet in terrane eclogites may have been produced by later H enrichments during their exhumation to the surface, e.g., by exchange with surrounding fluids. Such reactions may have further caused the heterogeneous distribution of water in sub-grain scales

of minerals in exhumed terrane eclogites (Xia et al. 2005; Sheng et al. 2007). It follows that, if this is the case, the recycling of water into the deep Earth would be controlled by other water carriers such as hydrous phases including the dense hydrous magnesium phases (DHMS), providing that a significant amount of water has indeed been recycled by subduction over geological scales. The persistence of hydrous assemblages in subducted slabs is critical for solving this problem. With subduction, some hydrous phases break down and release H₂O and new hydrous minerals might form, e.g., phlogopite and DHMS that are stable at greater depths than serpentine and amphibole which are important water carriers in the slabs at relatively shallow depths. The formation of hydrous minerals requires water-saturated (or at least water-abundant) conditions over a reasonable period. This requirement is, however, hard to satisfy, because the subducted slab and the released H₂O are usually not in a closed system. This actually raises open questions about whether new hydrous minerals could form at greater depths and whether they are of significant amounts. If the newly formed hydrous phases, if any, are only of a very small amount in subducted slabs, their ability to recycle water into the deep Earth would be very limited. Attention should be paid not only to how deep hydrous phases are stable, but also to how many their amounts are possible. This is beyond the scope of this study, and further work is required for clarifying these important issues.

Acknowledgements X.Y. thanks Stefan Keyssner for providing the starting eclogite. Editorial handling by Jochen Hoefs and comments by Fabrice Gaillard and the anonymous reviewers helped to improve the manuscript. This work was supported by the National Science Foundation of China (41725008 and 41590622) and National Basic Research Program of China (973 Project, 2014CB845904).

Appendix

End-member proportions of omphacite and garnet in eclogites from available reports and the starting minerals of this study are shown in Fig. 8. Among the various elements in dry pyroxenes and garnet, Fe affects greatly the conductivity of pyroxenes and garnet, and the composition of Fe is particularly emphasized in the plots. In general, omphacite and garnet are more abundant in Fe in terrane eclogites than in xenolith eclogites.

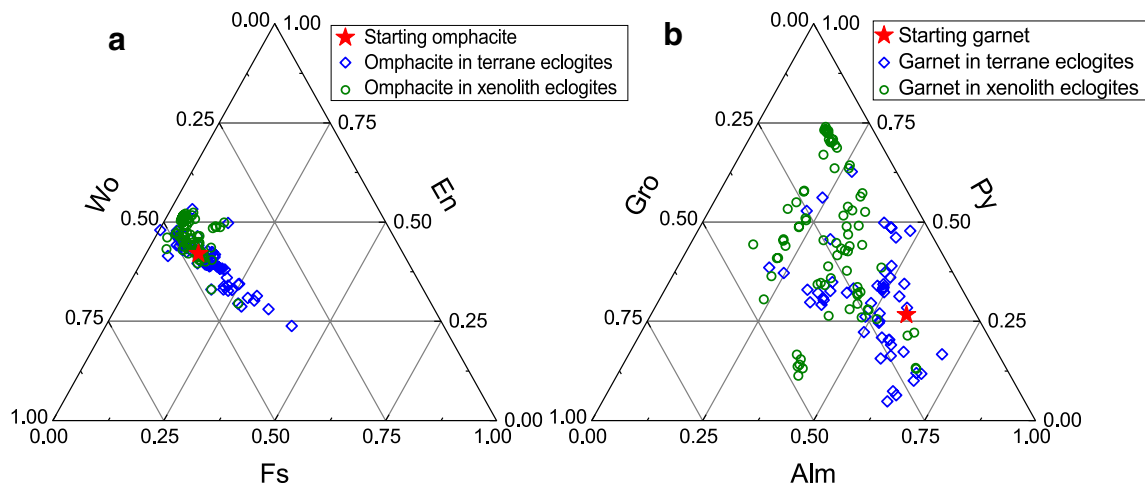


Fig. 8 End-member proportions of **a** omphacite and **b** garnet in eclogites. Data sources for terrane eclogites: Dabie-Sulu belt, China (Zhang et al. 2005; Sheng et al. 2007), Tien Shan, China (Zhang et al. 2002; Orozbaev et al. 2010; Bagdassarov et al. 2011), Alps (Rubatto and Hermann 2003), Bohemian Terrane, Central Europe (Kotková and Janák 2015), Papua New Guinea (Baldwin et al. 2004), West Norway (Jamtveit 1987), West Africa (Ménot and Sed-

doh 1985). Data sources for xenolith eclogites: Kaapvaal, South Africa (Jacob et al. 2009), Slave, Canada (Smart et al. 2009), Superior, Canada (Smit et al. 2014), Siberia, Russia (Pernet-Fisher et al. 2014), North China (Xu et al. 2006). Alm, almandite ($\text{Fe}_3\text{Al}_2\text{Si}_3\text{O}_{12}$), En, enstatite (MgSiO_3), Fs, ferrosilite (FeSiO_3), Gro, grossularite ($\text{Ca}_3\text{Al}_2\text{Si}_3\text{O}_{12}$), Pyp, pyrope ($\text{Mg}_3\text{Al}_2\text{Si}_3\text{O}_{12}$), Wo, wollastonite (CaSiO_3)

References

- Anderson DL (2007) The eclogite engine: chemical geodynamics as a Galileo thermometer. *Geol Soc Am Spec Pap* 430:47–64
- Austrheim H (1991) Eclogite formation and dynamics of crustal roots under continental collision zones. *Terra Nova* 3:492–499
- Bagdassarov N, Batalev V, Egorova V (2011) State of lithosphere beneath Tien Shan from petrology and electrical conductivity of xenoliths. *J Geophys Res* 116:B01202. <https://doi.org/10.1029/2009JB007125>
- Baldwin SL, Monteleone BD, Webb LE, Fitzgerald PG, Grove M, Hill EJ (2004) Pliocene eclogite exhumation at plate tectonic rates in eastern Papua New Guinea. *Nature* 431:263–267
- Chave AD, Constable SC, Edwards RN, Nabighian MN (1991) Electrical exploration methods for the seafloor. In: Nabighian MN (ed) *Electromagnetic methods in applied geophysics—volume 2, application*. Society of Exploration Geophysicists, Tulsa, pp 931–966
- Constable S (2006) SEO3: a new model of olivine electrical conductivity. *Geophys J Int* 166:435–437
- Dai L, Karato S-I (2009) Electrical conductivity of pyrope-rich garnet at high temperature and high pressure. *Phys Earth Planet Inter* 176:83–88
- Dai L, Hu H, Li H, Wu L, Hui K, Jiang J, Sun W (2016) Influence of temperature, pressure, and oxygen fugacity on the electrical conductivity of dry eclogite, and geophysical implications. *Geochem Geophys Geosyst* 17:2394–2407
- Evans RL, Hirth G, Baba K, Forsyth D, Chave A, Mackie R (2005) Geophysical evidence from the MELT area for compositional controls on oceanic plates. *Nature* 437:249–252
- Franz G, Thomas S, Smith DC (1986) High-pressure phengite decomposition in the Weissenstein eclogite, Münchberger Gneiss Massif, Germany. *Contrib Mineral Petrol* 92:71–85
- Frost D, McCammon C (2008) The redox state of the Earth's mantle. *Annu Rev Earth Planet Sci* 36:389–420
- Gardés E, Gaillard F, Tarits P (2014) Toward a unified hydrous olivine electrical conductivity law. *Geochem Geophys Geosyst* 15:4984–5000
- Giese P, Scheuber E, Schilling M, Schmitz M, Wigger P (1999) Crustal thickening processes in the central Andes and the different natures of the Moho-discontinuity. *J S Am Earth Sci* 12:201–220
- Glover P (1996) Graphite and electrical conductivity in the lower continental crust: a review. *Phys Chem Earth* 21:279–287
- Guo Y, Wang D, Shi Y, Zhou Y, Dong Y, Li C (2014) The electrical conductivity of eclogite in Tibet and its geophysical implications. *Sci China Earth Sci* 57:2071–2078
- Hashin Z, Shtrikman S (1963) A variational approach to the theory of the elastic behaviour of multiphase materials. *J Mech Phys Solid* 11:127–140
- Huang X, Xu Y, S-i Karato (2005) Water content in the transition zone from electrical conductivity of wadsleyite and ringwoodite. *Nature* 434:746–749
- Huebner JS, Dillenburg RG (1995) Impedance spectra of hot, dry silicate minerals and rock: qualitative interpretation of spectra. *Am Mineral* 80:46–64
- Hyndman RD, Shearer PM (1989) Water in the lower continental crust: modelling magnetotelluric and seismic reflection results. *Geophys J Int* 98:343–365
- Ingrin J, Blanchard M (2006) Diffusion of hydrogen in minerals. *Rev Mineral Geochem* 62:291–320
- Ingrin J, Skogby H (2000) Hydrogen in nominally anhydrous upper-mantle minerals: concentration levels and implications. *Eur J Mineral* 12:543–570
- Jacob DE (2004) Nature and origin of eclogite xenoliths from kimberlites. *Lithos* 77:295–316
- Jacob DE, Viljoen KS, Grassineau NV (2009) Eclogite xenoliths from Kimberley, South Africa—a case study of mantle metasomatism in eclogites. *Lithos* 112:1002–1013
- Jamtveit B (1987) Metamorphic evolution of the Eiksunddal eclogite complex, Western Norway, and some tectonic implications. *Contrib Mineral Petrol* 95:82–99
- Kapinos G, Montahaei M, Meqbel N, Brasse H (2016) Three-dimensional electrical resistivity image of the South-Central Chilean subduction zone. *Tectonophysics* 666:76–89

- Karato SI (1990) The role of hydrogen in the electrical conductivity of the upper mantle. *Nature* 347:272–273
- Katayama I, Nakashima S (2003) Hydroxyl in clinopyroxene from the deep subducted crust: evidence for H₂O transport into the mantle. *Am Mineral* 88:229–234
- Katayama I, Nakashima S, Yurimoto H (2006) Water content in natural eclogite and implication for water transport into the deep upper mantle. *Lithos* 86:245–259
- Kay RW, Mahlburg-Kay S (1991) Creation and destruction of lower continental crust. *Geol Rundsch* 80:259–278
- Kotková J, Janák M (2015) UHP kyanite eclogite associated with garnet peridotite and diamond-bearing granulite, northern Bohemian Massif. *Lithos* 226:255–264
- Li Y, Yang X, Yu JH, Cai YF (2016) Unusually high electrical conductivity of phlogopite: the possible role of fluorine and geophysical implications. *Contrib Mineral Petrol* 171:37. <https://doi.org/10.1007/s00410-016-1252-x>
- Li Y, Jiang H, Yang X (2017) Fluorine follows water: effect on electrical conductivity of silicate minerals by experimental constraints from phlogopite. *Geochim Cosmochim Acta* 217:16–27
- Liu H, Zhu Q, Yang X (2019) Electrical conductivity of fluorite and fluorine conduction. *Minerals* 9:72. <https://doi.org/10.3390/min9020072>
- Manning CE (2004) The chemistry of subduction-zone fluids. *Earth Planet Sci Lett* 223:1–16
- Manthilake G, Mookherjee M, Bolfan-Casanova N, Andraut D (2015) Electrical conductivity of lawsonite and dehydrating fluids at high pressures and temperatures. *Geophys Res Lett* 42:7398–7405
- McGary RS, Evans RL, Wannamaker PE, Elsenbeck J, Rondenay S (2014) Pathway from subducting slab to surface for melt and fluids beneath Mount Rainier. *Nature* 511:338–340
- Ménot RP, Seddoh KF (1985) The eclogites of the Lato hills, south Togo, West Africa: relics from the early tectonometamorphic evolution of the Pan-African orogeny. *Chem Geol* 50:313–330
- Orozbaev RT, Takasu A, Bakirov AB, Tagiri M, Sakiev KS (2010) Metamorphic history of eclogites and country rock gneisses in the Aktyuz area, Northern Tien-Shan, Kyrgyzstan: a record from initiation of subduction through to oceanic closure by continent–continent collision. *J Metamorph Geol* 28:317–339
- Pernet-Fisher JF, Howarth GH, Liu Y, Barry PH, Carmody L, Valley JW, Bodnar RJ, Spetsius ZV, Taylor LA (2014) Komsomolskaya diamondiferous eclogites: evidence for oceanic crustal protoliths. *Contrib Mineral Petrol* 167:981. <https://doi.org/10.1007/s00410-014-0981-y>
- Poe BT, Romano C, Nestola F, Smyth JR (2010) Electrical conductivity anisotropy of dry and hydrous olivine at 8 GPa. *Phys Earth Planet Inter* 181:103–111
- Qiu Y, Jiang H, István K, Xia Q, Yang X (2018) Quantitative analysis of H-species in anisotropic minerals by unpolarized infrared spectroscopy: an experimental evaluation. *Am Mineral* 103:1761–1769
- Reynard B, Mibe K, Van de Moortele B (2011) Electrical conductivity of the serpentinised mantle and fluid flow in subduction zones. *Earth Planet Sci Lett* 307:387–394
- Romano C, Poe BT, Kreidie N, McCammon CA (2006) Electrical conductivities of pyrope-almandine garnets up to 19 GPa and 1700 C. *Am Mineral* 91:1371–1377
- Rubatto D, Hermann J (2003) Zircon formation during fluid circulation in eclogites (Monviso, Western Alps): implications for Zr and Hf budget in subduction zones. *Geochim Cosmochim Acta* 67:2173–2187
- Shankland TJ, Ander ME (1983) Electrical conductivity, temperatures, and fluids in the lower crust. *J Geophys Res* 88:9475–9484
- Shankland TJ, O'Connell RJ, Waff HS (1981) Geophysical constraints on partial melt in the upper mantle. *Rev Geophys* 19:394–406
- Sheng YM, Xia QK, Dallai L, Yang XZ, Hao YT (2007) H₂O contents and D/H ratios of nominally anhydrous minerals from ultrahigh-pressure eclogites of the Dabie orogen, eastern China. *Geochim Cosmochim Acta* 71:2079–2103
- Shuai K, Yang X (2017) Quantitative analysis of H-species in anisotropic minerals by polarized infrared spectroscopy along three orthogonal directions. *Contrib Mineral Petrol* 172:14. <https://doi.org/10.1007/s00410-017-1336-2>
- Skogby H, Bell DR, Rossman GR (1990) Hydroxide in pyroxene—variations in the natural environment. *Am Mineral* 75:764–774
- Smart KA, Heaman LM, Chacko T, Simonetti A, Kopylova M, Mah D, Daniels D (2009) The origin of high-MgO diamond eclogites from the Jericho Kimberlite, Canada. *Earth Planet Sci Lett* 284:527–537
- Smit KV, Stachel T, Creaser RA, Ickert RB, DuFrane SA, Stern RA, Seller M (2014) Origin of eclogite and pyroxenite xenoliths from the Victor kimberlite, Canada, and implications for Superior craton formation. *Geochim Cosmochim Acta* 125:308–337
- Wang D, Mookherjee M, Xu Y, S-i Karato (2006) The effect of water on the electrical conductivity of olivine. *Nature* 443:977–980
- Wei W, Unsworth MJ, Jones AG, Booker J, Tan H, Nelson D, Chen L, Li S, Solon K, Bedrosian P, Jin S, Deng M, Ledo JJ, Kay D, Roberts B (2001) Detection of widespread fluids in the Tibetan crust by magnetotelluric studies. *Science* 292:716–718
- Wendlandt RF, Huebner JS, Harrison WJ (1982) The redox potential of boron nitride and implications for its use as a crucible material in experimental petrology. *Am Mineral* 67:170–174
- Xia QK, Sheng YM, Yang XZ, Yu HM (2005) Heterogeneity of water in garnets from UHP eclogites, eastern Dabieshan, China. *Chem Geol* 224:237–246
- Xu Y, Shankland TJ, Duba AG (2000a) Pressure effect on electrical conductivity of mantle olivine. *Phys Earth Planet Inter* 118:149–161
- Xu Y, Shankland TJ, Poe BT (2000b) Laboratory-based electrical conductivity in the Earth's mantle. *J Geophys Res* 105:27865–27875
- Xu W, Gao S, Wang Q, Wang D, Liu Y (2006) Mesozoic crustal thickening of the eastern North China craton: evidence from eclogite xenoliths and petrologic implications. *Geology* 34:721–724
- Xu Y, Zhang S, Griffin WL, Yang Y, Yang B, Luo Y, Zhu L, Afonso JC, Lei B (2016) How did the Dabie Orogen collapse? Insights from 3-D magnetotelluric imaging of profile data. *J Geophys Res* 121:5169–5185
- Yang X (2012) Orientation-related electrical conductivity of hydrous olivine, clinopyroxene and plagioclase and implications for the structure of the lower continental crust and uppermost mantle. *Earth Planet Sci Lett* 317:241–250
- Yang X, Heidelberg F (2012) Grain size effect on the electrical conductivity of clinopyroxene. *Contrib Mineral Petrol* 163:939–947
- Yang X, McCammon C (2012) Fe³⁺-rich augite and high electrical conductivity in the deep lithosphere. *Geology* 40:131–134
- Yang X, Deloule E, Xia Q, Fan Q, Feng M (2008) Water contrast between Precambrian and Phanerozoic continental lower crust in eastern China. *J Geophys Res* 113:B04208. <https://doi.org/10.1029/2007JB005541>
- Yang X, Keppler H, McCammon C, Ni H, Xia Q, Fan Q (2011) Effect of water on the electrical conductivity of lower crustal clinopyroxene. *J Geophys Res* 116:B04208. <https://doi.org/10.1029/2010JB008010>
- Yang X, Keppler H, McCammon C, Ni H (2012) Electrical conductivity of orthopyroxene and plagioclase in the lower crust. *Contrib Mineral Petrol* 163:33–48
- Yaxley GM, Green DH (1998) Reactions between eclogite and peridotite: mantle refertilisation by subduction of oceanic crust. *Schweiz Mineral Petrogr Mitt* 78:243–255
- Yoshino T, Manthilake G, Matsuzaki T, Katsura T (2008) Dry mantle transition zone inferred from the conductivity of wadsleyite and ringwoodite. *Nature* 451:326–329

- Yoshino T, Matsuzaki T, Shatskiy A, Katsura T (2009) The effect of water on the electrical conductivity of olivine aggregates and its implications for the electrical structure of the upper mantle. *Earth Planet Sci Lett* 288:291–300
- Zhang L, Ellis DJ, Williams S, Jiang W (2002) Ultra-high pressure metamorphism in western Tianshan, China: part II. Evidence from magnesite in eclogite. *Am Mineral* 87:861–866
- Zhang RY, Liou JG, Zheng J-P, Griffin WL, Yui TF, O'Reilly SY (2005) Petrogenesis of the Yangkou layered garnet-peridotite complex, Sulu UHP terrane, China. *Am Mineral* 90:801–813
- Zhao C, Yoshino T (2016) Electrical conductivity of mantle clinopyroxene as a function of water content and its implication on electrical structure of uppermost mantle. *Earth Planet Sci Lett* 447:1–9
- Zheng Y (2008) A perspective view on ultrahigh-pressure metamorphism and continental collision in the Dabie-Sulu orogenic belt. *Chin Sci Bull* 53:3081–3104

Publisher's Note Springer Nature remains neutral with regard to jurisdictional claims in published maps and institutional affiliations.